Int. J. Electrochem. Sci., 11 **(2016)** 80 - 94

International Journal of
ELECTROCHEMICAL
SCIENCE
www.electrochemsci.org

Effect of Hydroxyethil imidazoline and Ag Nanoparticles on the CO_2 Corrosion of Carbon Steel

L.M. Rivera-Grau[1], *J.G. Gonzalez-Rodriguez*[1,*], *L. Martinez*[2]

[1] Universidad Autonoma del Estado de Morelos, CIICAp, AV. Universidad 1001, 62209-Cuernavaca, Mor., Mexico
[2] Universidad Nacional Autonoma de Mexico, Instituto de Ciencias Fisicas, AV. Universidad s/n, Cuernavaca, Mor., Mexico
[*]E-mail: ggonzalez@uaem.mx

Received: 20 August 2015 / *Accepted:* 11 September 2015 / *Published:* 1 December 2015

An hydroxyetyl-imidazoline (HEI) has been used in conjunction with Ag nanoparticles and as CO_2 corrosion inhibitors for carbon steel in 3% NaCl+diesel solution at 50°C. Testing techniques includes linear polarization resistance, electrochemical impedance spectroscopy, and electrochemical noise measurements by using 20 ppm of inhibitor. Results indicated that the addition of Ag nanoparticles increased the steel corrosion rate, whereas the addition of HEI decreased it. When both Ag nanoparticlces anad HEI were added, the corrosion rate was slightly higher than that with HEI alone. Results are discussed in terms of the adsorption of Ag nanoparticles on sites not covered by the HEI formed film, and the formation of galvanic cells between silver and the steel surface.

Keywords: Acid corrosion, carbon steel, electrochemical noise.

1. INTRODUCTION

Carbon dioxide (CO_2) is present in trace levels up to 50% in oil and gas [1,2]. Besides, CO_2 could be intentionally added as part of secondary enhanced oil recovery processes and it is very corrosive to carbon and low alloy steel tubulars employed in the process equipment in this industry and it has become of great concern mainly to the increasing production of water for enhanced oil recovery [3]. Due to its economical impact in the oil and gas industry around the world, CO_2 corrosion has led to the application of many corrosion control methods and research. One of the most widely used methods is the injection of organic inhibitors into oil wells and pipelines [4,5]. Organic inhibitors such as imidazoline and its derivatives are among the most widely used inhibitors, which have been shown to be effective in oil and gas pipelines [6,7]. It is generally accepted that organic molecules inhibit

corrosion via adsorption at the metal–solution interface. The mode of adsorption is dependent on the following factors: structure of the molecule [8,9] solution chemistry [10,11] characteristics of the metal surface [12-14] electrochemical potential at the interface [15] the presence of a surfactant [16] among others.

A very dangerous forms of metals degradation which occurs in industries such as petroleum and gas is microbiologically influenced corrosion (MIC), and the use of biocides is necessary [16-20]. For a long time,centuries silver has been in used for the treatment of burns and chronic wounds. It has been used to make drinkable water since 1000 B.C. silver was used to make water potable. This is the reason why compounds based on silver have been used extensively in many bactericidal applications [16,17]. Some inorganic composites with a slow silver release rate are used at present days as preservatives in a variety of products; another application includes new compounds with silica gel microspheres, that are mixed into plastics for antibacterial protection [18, 19]. Some other compounds made of Silver are used in the medical field to treat burns and a variety of infections [20, 21]. It is very well known the bactericidal effect of silver ions on micro-organisms but the bactericidal mechanism is not wholly understood. It is believed that ionic silver inactivates vital enzymes [22- 24].

Synergistic inhibition, which is a method to improve the individual performance of a an inhibitor, several inhibitors, inhibitor with surfactants, or inhibitor + in order to prevent the corrosion of metals, has proved to be an effective method to decrease the amount of the tested inhibitor. Ramesh [24] performed polarization and impedance measurements on copper in neutral aqueous solution with and without inhibitors and biocide. The inhibitors used were 3-benzylidene amino 1,2,4-triazole phosphonate, 3-cinnamalidene amino 1,2,4-triazole phosphonate, 3-salicylalidene amino 1,2,4-triazole phosphonate and 3-paranitro benzylidene amino 1,2,4-triazole phosphonate (PBATP). The effect of inhibitors and biocide against the corrosion of copper in neutral aqueous solution has been studied. Zhao et al. [25] investigated the corrosion inhibition of a quinolinium quaternary ammonium salt and a Gemini surfactant, 1,3-bis(dodecyldimethylammonium chloride)-2-propanol, for mild steel in H_2S and CO_2 saturated brine solution by using polarization test, EIS and XPS studies. The synergistic effect is found between these two compounds when the Gemini concentration is less than 50 mg L^{-1} in the solution containing 100 mg L^{-1} quinolinium quaternary ammonium salt, and it disappears when the Gemini concentration is larger than 50 mg L^{-1}. The synergistic mechanism is explained by competitive adsorption of these two compounds on steel surface. Zheng [26] evaluated the corrosion inhibition of oleic-based imidazoline (OIM) and sodium benzoate (SB) on mild steel in a CO_2-saturated solution by using a weight-loss method and a potentiodynamic polarization technique. The results show that OIM can protect mild steel from CO_2 corrosion to some extent, and its inhibition can be strengthened by using it in combination with SB. The synergistic inhibition effect of OIM and SB was obvious. Thus, the goal of this work is to evaluate the synergistic action of an organic inhibitor with Ag nanoparticles in the corrosion of carbon steel in a CO_2-environement.

2. EXPERIMENTAL PROCEDURE

Testing material includes a 1018 carbon steel. Coupons in cylindrical shape, 10 mm long with a diameter of 6 mm were machined and embedded in PTFE exposing an effective surface area of 0.28

cm^2 to the electrolyte. They were ground with 2400 grade emery paper, rinsed with distilled water, acetone, and dried under an air flow. Testing solution consisted of 3 wt.% NaCl as base solution. To this solution, 10 vol.% diesel oil was added. Organic used inhibitor included an hydroxyethyl imidazoline (HEI), from Lakeland Labs. (U.K.),with a molecular structure as shown in Fig. 1, in a concentration of 10 ppm.

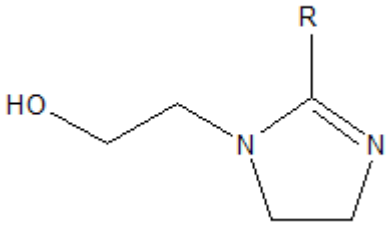

Figure 1. Chemical struture of hydroxyetyl-imidazoline (HEI), where R is an ethyl group.

Solutions were saturated with CO_2 (99.9%) during 2 h before testing and kept under a CO_2 atmosphere during testing. For all experiments, the system temperature was maintained constant at 50 ± 2 ºC. The test solution was further stirred by using a rotating magnet at the bottom of the cell. The electrode was allowed to pre-corrode in the corrosive electrolyte for 2 h before the inhibitor was introduced. Commercial Ag nanoparticles were used as biocide in a concentration of 12.5 ppm. Once either the inhibitor, or the biocide or both were added to the solution, a time of 30 minutes was allowed to the solution before the measurements were taken.

Electrochemical measurements included linear polarization resistance (LPR), electrochemical noise (EN) and electrochemical impedance spectroscopy (EIS) measurements. Electrochemical tests ts were obtained in a glass cell by using graphite rod and a saturated calomel (SCE) as auxiliary and reference electrode respectively as using a conventional three electrode glass cell with two graphite rods as auxiliary electrodes. LPR reading were taken by polarizing the specimen ±10 mV_{SCE} around E_{corr} at a scanning rate of 1 mV/s every 60 minutes, during 24 hours. During the LPR tests, the E_{corr} value was monitored also. EIS tests were carried out at the E_{corr} value by using a signal with amplitude of 10 mV_{SCE} and a frequency interval of 0.1 Hz-30 kHz. An ACM potentiostat controlled by a desk top computer was used for the LPR tests and polarization curves, whereas for the EIS measurements a PC4 300 Gamry potentiostat was used. EN measurements were made by recording simultaneously the potential and current fluctuations at a sampling rate of 1 point per second in blocks of 1024 readings using two nominally identical working electrodes, and a SCE reference electrode. EN measurements every 60 minutes. For this, a zero resistance ammeter (ZRA) was used. A least square fitting method was used for the removal of the DC trend. To calculate the noise resistance, $R_{n,}$ the ratio of the potential noise standard deviation, $\sigma_{v,}$ over the current noise standard deviation, σ_i, was used according to Eq. [1]:

$$R_n = \sigma_v/\sigma_i \quad [1]$$

where R_n can be taken as the linear polarization resistance, R_p in the Stern-Geary equation:

$$i_{corr} = \frac{b_a b_c}{2.3(b_a + b_c)} \frac{1}{R_P} \quad [2]$$

thus, inversely proportional to the corrosion corrosion current density, i_{corr}, but with the necessary condition that a trend removal applied over an average baseline, as previously established [26].

3. RESULTS AND DISCUSSION

Although the potential shift vs time in Fig. 2 can provide some information about the corrosion mechanism, corrosion potential shift does not necessarily have any correlation with the corrosion rate. The change in the E_{corr} value with time for the different systems is shown in Fig. 2, where it can be seen that, for the base CO_2+diesel-saturated NaCl solution, the E_{corr} value is close to -750 mV, and it shifts towards slightly nobler values, reaching a value of -730 mV after 24 hours of testing.

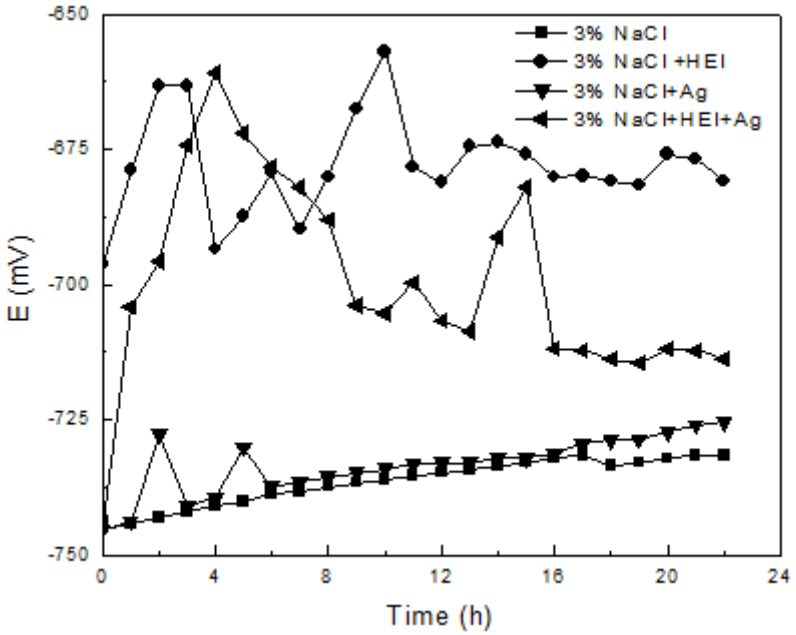

Figure 2. Variation of the E_{corr} value with tme for carbon steel in a CO_2-saturated 3% NaCl+diesel solution containing HEI and Ag nanoparticles.

This value practically did not change with the addition of silver nanoparticles, but when either the HEI alone or HEI+Ag nanoparticles were added, the E_{corr} became nobler, between -700 and -660 mV. During the first hours of testing, the E_{corr} value became nobler that at the beginning of the test in both cases, but it became more or less constant, around -675 mV in the case of the addition of HEI. When both additives were added together, the E_{corr} shifted towards more active values after reaching a peak value close to -660 mV. Thus, the noblest E_{corr} value was reached with the addition of inhibitor HEI, maybe due to its adsorption on the steel surface [7-14]. The changes of corrosion potential

indicate that the carbon steel is harder to dissolution after the use of either HEI or the combined use of HEI+Ag nanoparticles.

The change in the polarization resistance vale (R_p) with time for the different systems is plotted in Fig. 3.

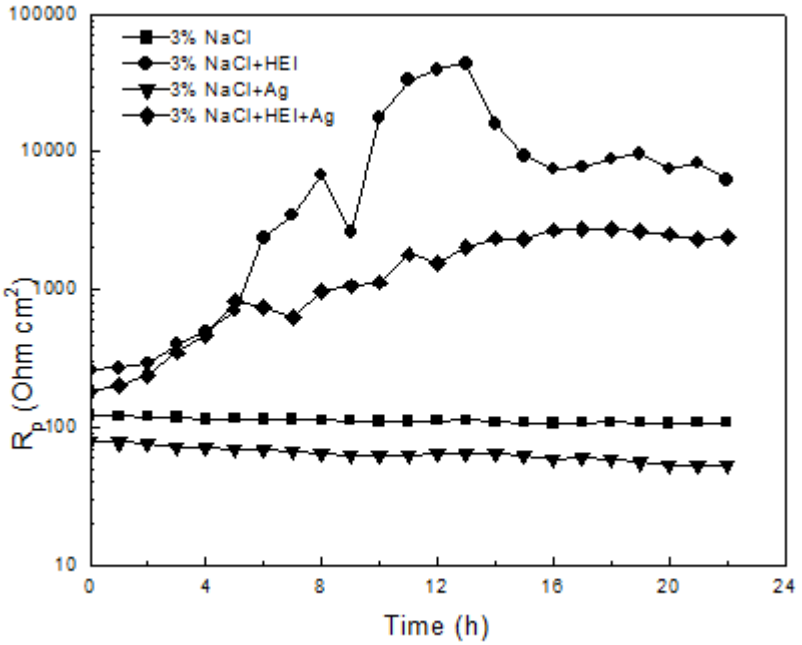

Figure 3. Variation of the R_p value with time for carbon steel in a CO_2-saturated 3% NaCl+diesel solution containing HEI and Ag nanoparticles.

It can be seen that the lowest R_p value, around 100 ohm cm^2, and thus the highest corrosion rate, was obtained for the base, uninhibited CO_2+diesel-saturated NaCl solution or when the silver nanoparticles were added. When silver nanoparticles + HEI were added together, the R_p value increased as time elapsed, reaching a value close to 2 000 ohm cm^2 after 15 hours or so, and remained constant until the end of the test. However, when only HEI was added alone, the R_p value increased with time and reached a value higher than 50 000 ohm cm^2 after 12 hours of testing, but decreased down to 10 000 ohm cm^2. This increase in the R_p value might be due to the adsorption of HEI inhibitor and the formation of a protective layer [7-14]. It is very well known that in CO_2 environments, iron and steel form an external layer of iron carbonate, $FeCO_3$ [27].According to its homogeneity, porosity, tenacity, thickness, adherence and nature of the corrosion layer, it can be protective or not [28-31]. When the inhibitor is added, a complex formed by iron ions, Fe^{2+} and the inhibitor on the steel surface, which is compact, adherent, not soluble, protects the steel from further corrosion by the electrolyte. The resulting complex could, depending on its relative solubility, either inhibit or catalyze further metal dissolution [32]. Thus, the lowest corrosion rate was obtained with the addition of HEI. However, when silver nanoparticles are added together with inhibitor HEI, the R_p value obtained with HEI decreased, increasing, thus, the steel corrosion rate, which could be due to a decrease in the

covered metal surface by inhibitor or to the co-adsorption of the silver nanoparticles and the formation of micro-galvanic cells between iron and Ag.

Inhibitor efficiency values were calculated (E) with equation

$$E(\%) = \frac{R_{p,i} - R_{p,b}}{R_{p,i}} \text{ X } 100 \qquad [3]$$

where $R_{p,b}$ is the linear polarization resistance without inhibitor and $R_{p,i}$ is the linear polarization resistance with inhibitor. Results, plotted in Fig. 4, show that the highest inhibitor efficiency was obtained with the addition of HEI, with values close to 99 %.

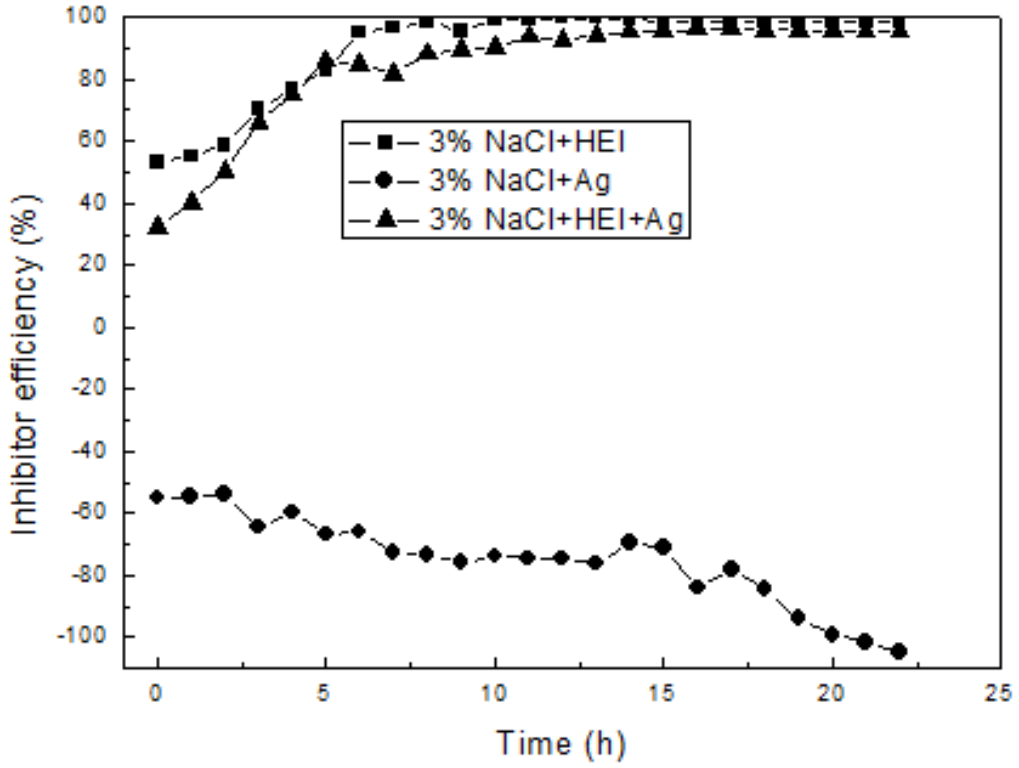

Figure 4. Calculated inhibitor efficiency values by using the R_p results.

This value started close to 55 % at the beginning of the experiment, but as time elapsed it increased up to 99 %, which is due to the increase in the inhibitor covered area of the steel surface. As can be seen from Fig. 4, the lowest inhibitor efficiency was obtained with the Ag nanoparticles were added, obtaining even negative efficiency values, which means that the addition of these particles increased the steel corrosion rate maybe due to a galvanic effect between the Ag particles and the steel. Silver is normally nobler than steel, therefore, when they are coupled together, steel will act as anode. When both Ag nanoparticles and HEI are added together, the inhibitor efficiency is lower than that obtained with HEI only, making clear the detrimental effect of the nanoparticles.

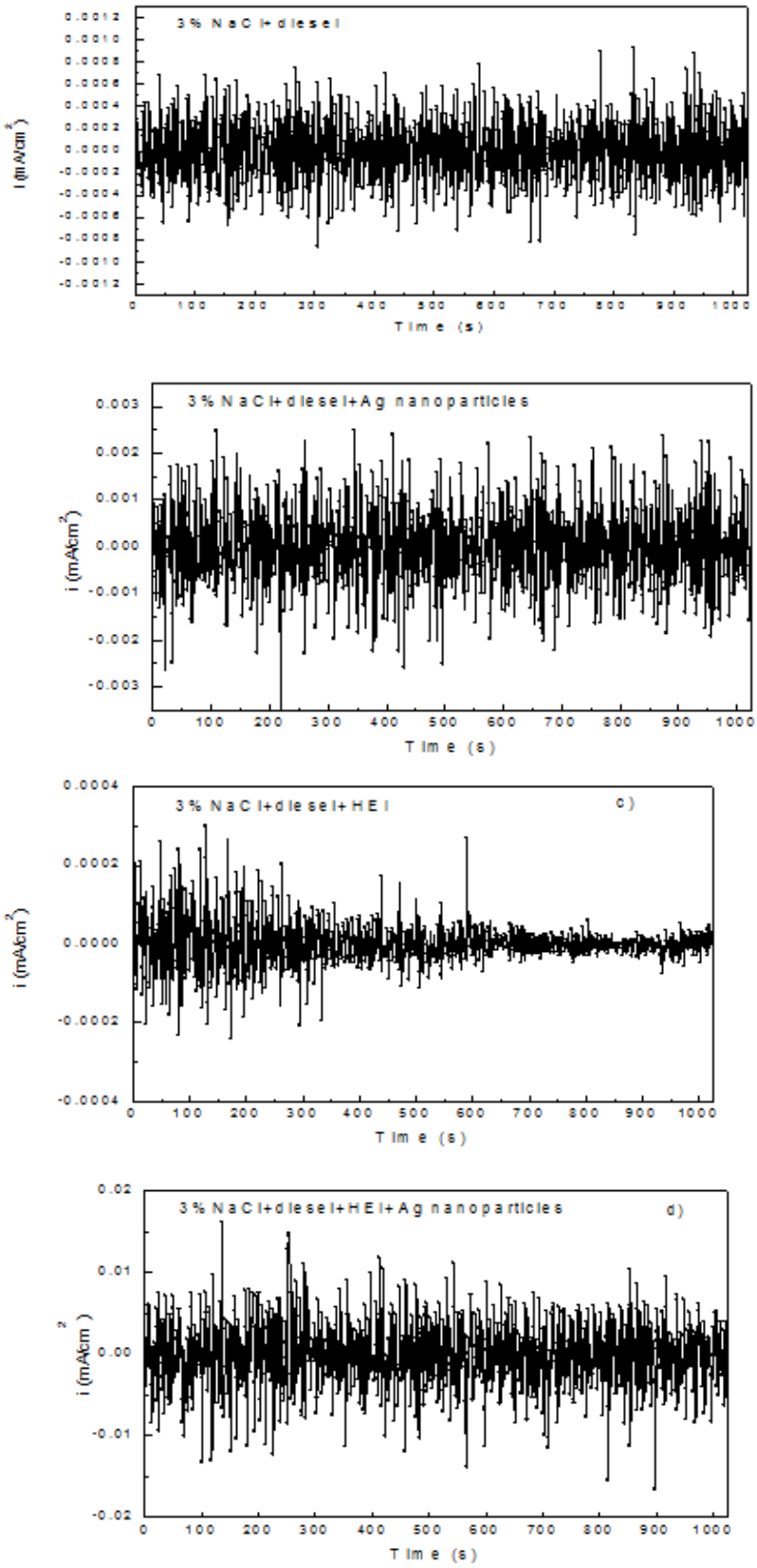

Figure 5. Time series for the noise in current obtained for carbon steel in a CO_2-saturated 3% NaCl+diesel solution containing HEI and Ag nanoparticles.

Noise in current for the different studied systems is given in Fig. 5 a-d respectively. For the base CO_2+diesel-saturated NaCl solution and the one containing silver nanoparticles, Fig, 5 a and b, time series consisted of current transients with high frequency and high intensity, typical of a metal undergoing a uniform type of corrosion [33]. However, the intensity or magnitude of the current transients obtained with the addition of silver nanoparticles was higher than that obtained for the base NaCl solution, indicating a higher corrosion rate. When HEI inhibitor was added, Fig. 5 c, the observed current transients had a lower intensity than that observed in presence of the silver nanoparticles or with the uninhibited solution, indicating a lower corrosion rate. These transients are due to the rupture of the HEI-formed film and to its re-healing or to the fact that some places of the steel surface are not covered by this film. As time elapsed, the current intensity or amplitude decreased continuously, which indicates that the corrosion rate decreases as time elapses due to the adsorption of inhibitor. It seems that the continuous decrease in current noise may correspond with the formation of the inhibitor film.

When both HEI and silver nanoparticles were added, Fig. 5 d, current transients with high intensity, in fact the highest current density intensity observed, indicating a high corrosion rate, the highest corrosion rate obtained so far, higher than that obtained with the addition of HEI only, which means that the addition of the silver nanoparticles increased the corrosion rate. Thus, the addition of inhibitor decreases the corrosion rate, but when silver nanoparticles and the inhibitor are added together, an increase in the corrosion rate is observed as reported in the results given above.

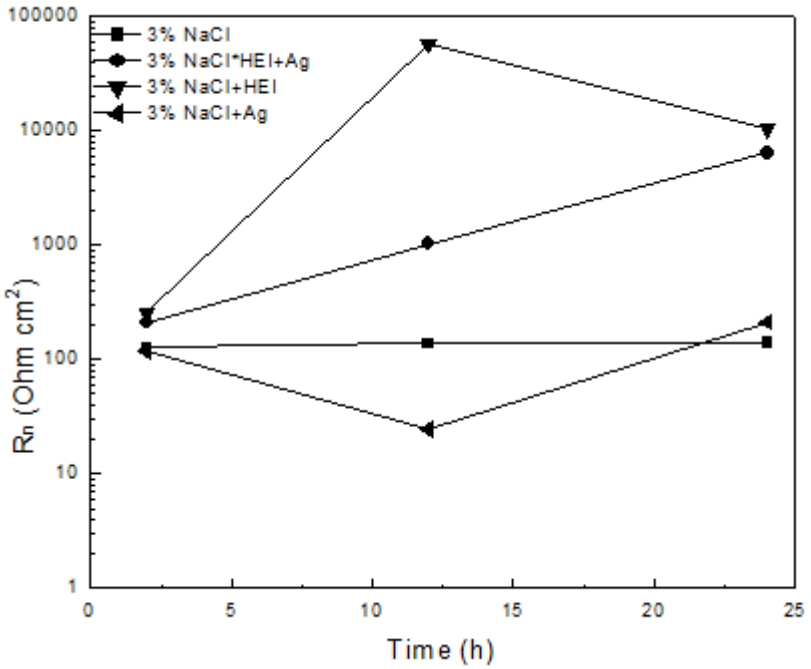

Figure 6. Variation of the R_n value with time for carbon steel in a CO_2-saturated 3% NaCl+diesel solution containing HEI and Ag nanoparticles.

An exact relationship between current noise and the corrosion process has not yet been found even when the current noise obviously correlates with the inhibitor filming process. However, the ratio of the standard deviation of voltage noise and the standard deviation of current noise, th noise

resistance (R_n), was found to be comparable to the polarization resistance and could be used to calculate the corrosion rate [34]. This was confirmed when the noise resistance value, R_n, was obtained by using Eq.[1] and the results are plotted in Fig. 6 at 0, 12 and 24 hours of testing. This figure shows that the lowest R_n values were obtained for the uninhibited CO_2+diesel-saturated NaCl solution and when the silver nanoparticles were added. On the other hand, the highest R_n value was obtained when the HEI inhibitor was added alone, obtaining a value close to 50 000 ohm cm^2, very similar to the R_p values obtained in Fig. 3. Once again, when both the silver nanoparticles and HEI inhibitor were added together an increase in the corrosion rate, as compared to that obtained with HEI only, in agreement with the LPR results.

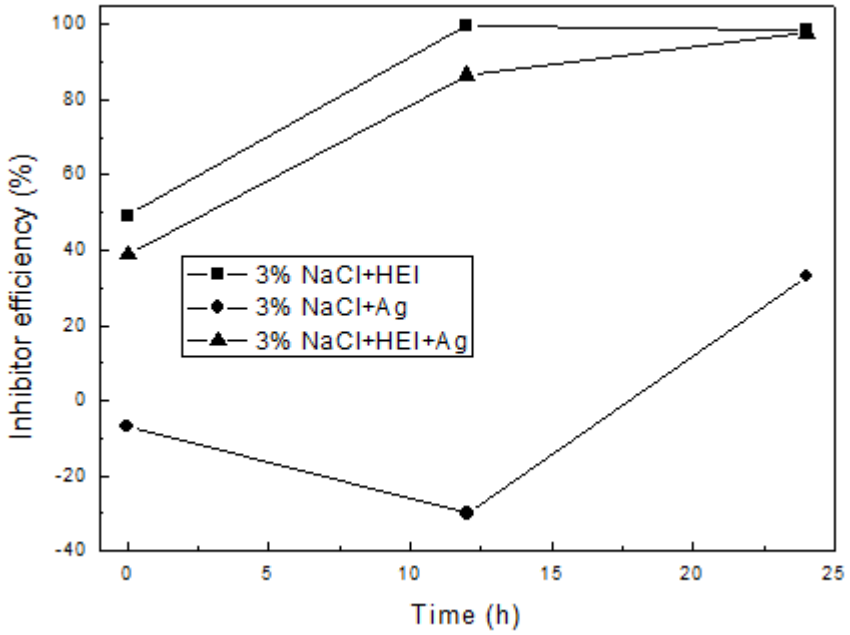

Figure 7. Calculated inhibitor efficiency values by using the R_p results.

Inhibitor efficiency calculated by using the noise resistance values were calculated by using eq. [3] but instead of R_p we use the noise resistance value, R_n, and the obtained results are shown in Fig. 7, which, similar to the results obtained with the polarization resistance results, Fig. 4, show that the highest inhibitor efficiency values were obtained with the addition of HEI alone, whereas the lowest values were obtained with the addition of silver nanoparticles. Once again, the addition of HEI and silver nanoparticles together decreased the inhibitor efficiency values obtained with the addition of HEI alone. Thus, different techniques gave similar results. Tan et al. [36] used electrochemical noise analysis, in both current and voltage, to monitor continuously the film formation and destruction processes of carbon dioxide corrosion inhibitor imidazoline. Our results showed that the noise resistance (R_n) was directly correlated to polarization resistance (R_p) and effectively followed the inhibitor film formation and destruction processes and found that following the same trend with inhibitor concentration and time.

Nyquist diagrams for the uninhibited uninhibited base CO_2+diesel-saturated NaCl solution is given in Fig. 8. This figure shows that data displayed a single, depressed, capacitive-like semicircle with its center in the real axis.

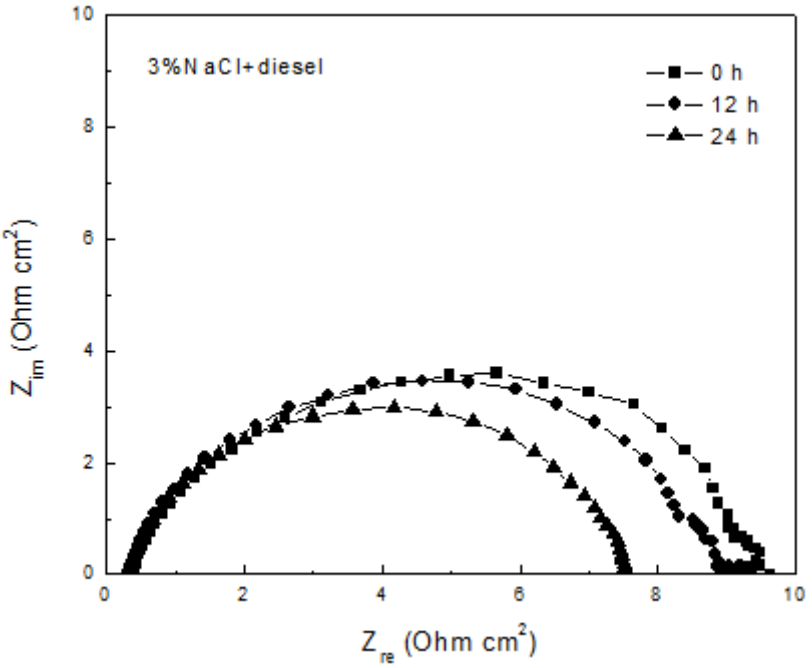

Figure 8. Nyquist diagrams for carbon steel in a CO_2-saturated 3% NaCl+diesel solution.

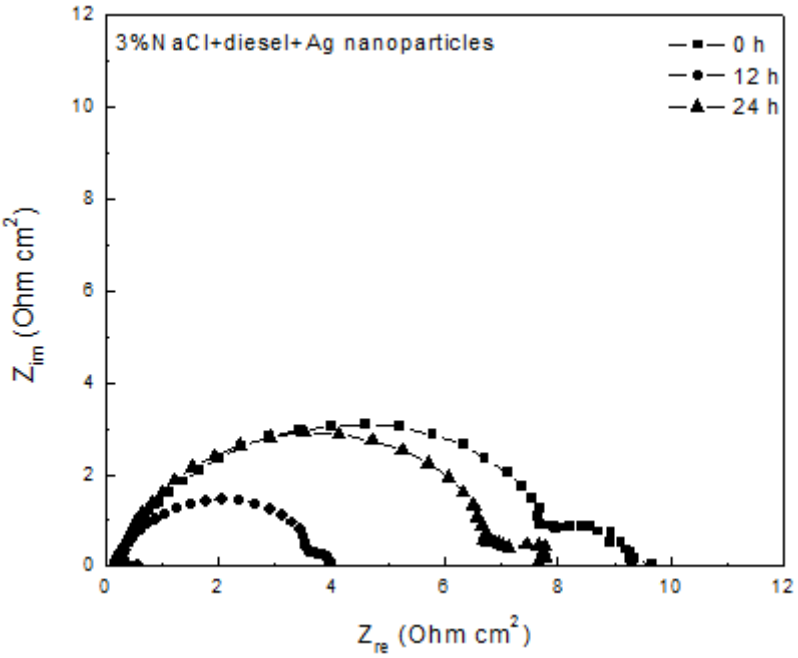

Figure 9. Nyquist diagrams for carbon steel in a CO_2-saturated 3% NaCl+diesel solution containing Ag nanoparticles.

This indicates that the corrosion process is under charge transfer control. This semicircle has been attributed to the formation and growth of a $FeCO_3$ film [27]. As time elapsed, the semicircle

diameter, its charge transfer resistance, R_{ct}, decreased which is due to the dissolution of the iron carbonate film, indicating its non-protective nature. The R_{ct} value can be calculated as the real value of the impedance when the imaginary part is equal to cero. When the silver nanoparticles were added, Fig. 9, data displayed, at high and intermediate frequency values, a depressed, capacitive-like and at lower frequencies, a second one, indicating a corrosion process controlled by the charge transfer.

The first high frequency semicircle is related to the formation of the $FeCO_3$ film, whereas the second one is related with the co-adsorption of silver nanoparticles and the formation of a second layer. The semicircle diameter had a slightly lower value than that obtained for the uninhibited solution, indicating that the addition of the silver nanoparticles increases the corrosion rate.

Nyquist diagrams for the CO_2-saturated NaCl solution with the addition of inhibitor HEI, Fig. 10, displayed a depressed, capacitive semicircle at high and intermediate frequency values followed by a straight line at low frequencies at the beginning of the test. This indicates that corrosion process is under controlled by a charge transfer and by the aggressive species diffusion. For longer times, data displayed a single capacitive semicircle, which indicates charge transfer-controlled process.

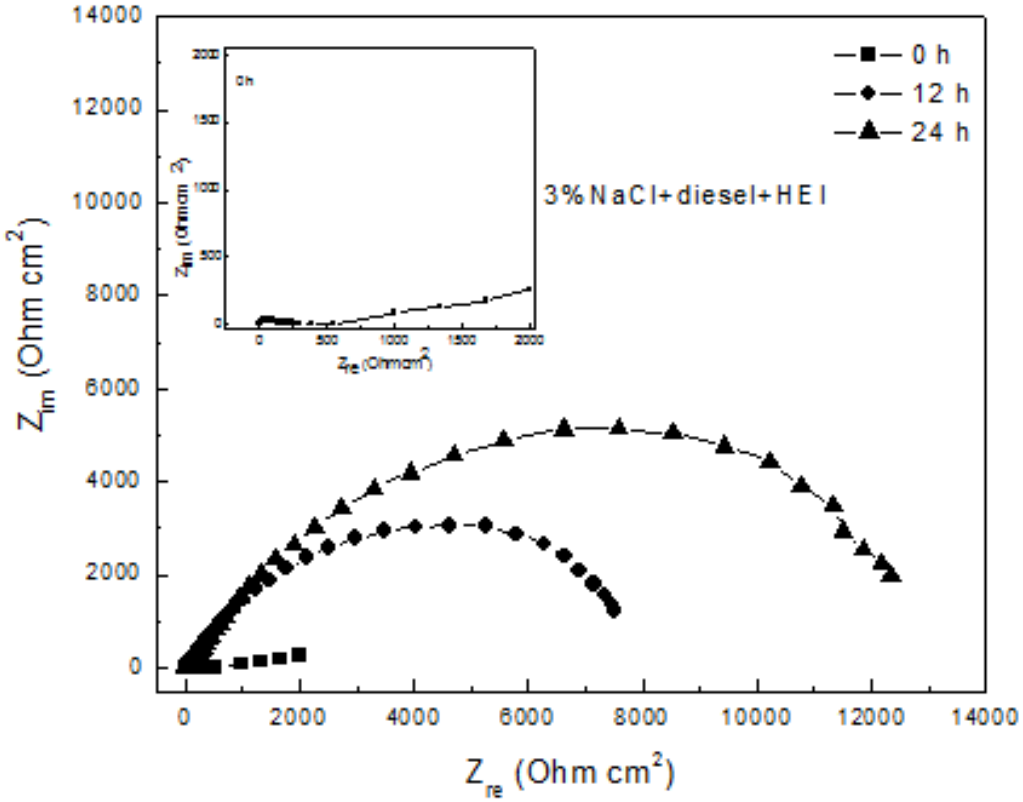

Figure 10. Nyquist diagrams for carbon steel in a CO_2-saturated 3% NaCl+diesel solution containing HEI inhibitor.

However, the R_{ct} value is around 12 000 ohm cm^2, the highest value shown so far, and it decreased down to 8000 ohm cm^2 after 24 hours of testing. Therefore, the lowest corrosion rate was obtained with the addition of inhibitor HEI.

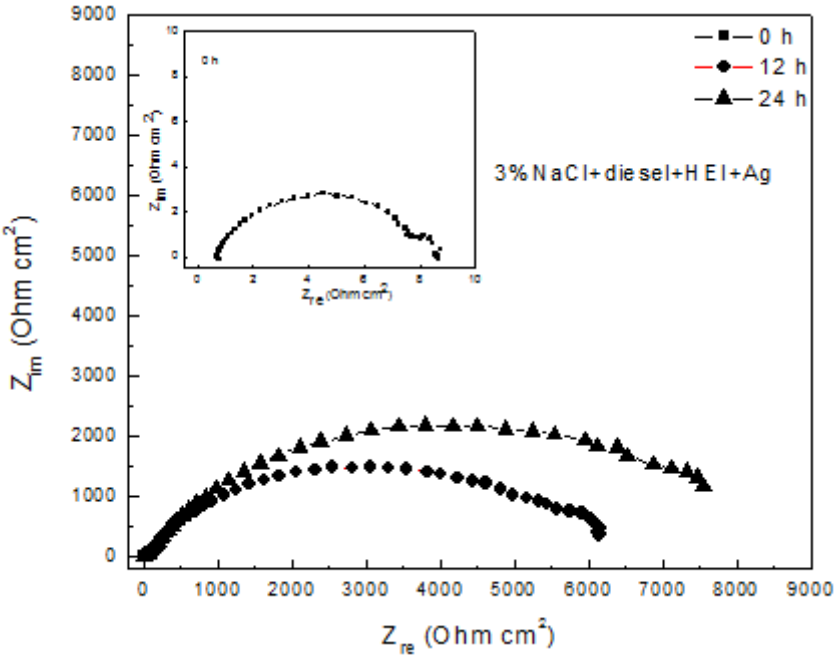

Figure 11. Nyquist diagrams for carbon steel in a CO_2-saturated 3% NaCl+diesel solution containing HEI +Ag anoparticles.

Finally, Nyquist data for the CO_2-saturated NaCl solution with the addition of both silver nanoparticles and inhibitor HEI, Fig. 11, displayed a depressed, capacitive semicircle at high and intermediate frequency values, followed by a second capacitive semicircle at lower frequency values at the beginning of the experiment, very similar to that shown for the solution with the addition of silver nanoparticles,

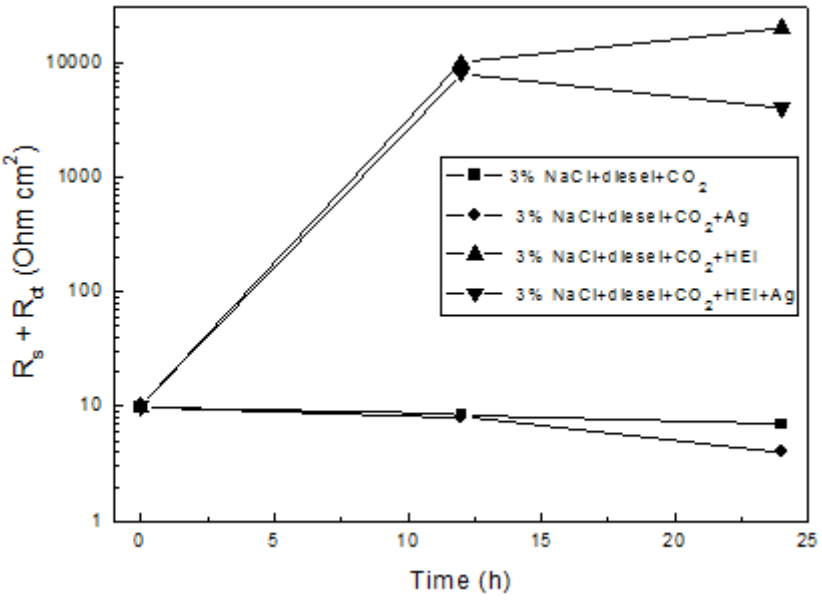

Figure 12. Variation of the R_s+R_{ct} value with time for carbon steel in a CO_2-saturated 3% NaCl+diesel solution containing HEI and Ag nanoparticles

Fig. 9. The high frequency loop diameter was very small, around 7 ohm cm^2, whereas that for the second, low frequency semicircle is less than 2 ohm cm^2, as that found for the semicircle displayed in solution with the addition of silver nanoparticles. As time elapsed, data displayed a depressed, capacitive semicircle at all frequency values, and the semicircle diameter decreased towards the end of the test, increasing, thus, the corrosion rate. The shape of these capacitive semicircles resembles those obtained when inhibitor HEI was added, Fig. 10.

During the monitoring of the formation and destruction of corrosion inhibitor films using electrochemical noise analysis, Tan et al. [36] found that the noise resistance value, R_n, polarization resistance, R_p, and the charge transfer resistance the inhibitor film resistance, $R_{ct}+R_f$ were directly correlated. In this case, $R_{ct}+R_f$ were calculated by semicircle fitting of EIS Nyquist plots. Results are plotted in Fig. 12. It can be seen that the lowest $R_{ct}+R_f$ value was for the uninhibited solution or with the addition of silver nanoparticles, whereas the highest values were obtained with the addition of inhibitor or with the inhibitor +the silver nanoprticles, although towards the end of the test, the highest value was that obtained with the addition of inhibitor alone. These values were smaller than those exhibited by R_p and R_n (Figs. 3 and 6 respectively) but the trend was the same.

On the other hand, the double layer capacitance, C_{dl}, and the charge transfer resistance value, R_{ct}, are related by following equation [36]:

$$C_{dl} = (2\pi f_{max} R_{ct})^{-1} \quad [4]$$

where f_{max} is the frequency value at which the imaginary component of the impedance is maximal.

Table 1. Electrochemical parameters calculated from EIS data for carbon steel after 12 h of immersion in a CO_2-saturated 3%NaCl+diesel containing HEI and Ag nanoparticles.

System	f_{max}(Hz)	R_{ct}(Ohm cm^2)	C_{dl}(μF cm^{-2})
3%NaCl+diesel+CO_2	31	9	576
3%NaCl+diesel +CO_2+Ag	9	35	501
3%NaCl+diesel +CO_2+HEI	83	10070	14
3%NaCl+diesel +CO_2+HEI+Ag nanoprticles	31	7560	20

By using the R_{ct} values obtained from Figs. 8-11, the calculated C_{dl} values are given in table 1. It is clear the increase in the R_{ct} value with the addition of HEI after 12 hours of exposure to the aggressive solution brings a decrease in the capacitance value. This is due to the displacement of the aggressive molecules by the inhibitors molecules on the steel surface. As time elapsed, the molecules of the inhibitor are desorbed from the metal, leaving the metal exposed to the electrolyte and increasing the corrosion rate. The addition of the Ag nanoparticles practically did not affect the C_{dl} value of the uninhibited base solution, but when they were added together with HEI inhibitor, the C_{dl}

value was similar, but slightly higher than that obtained when only HEI was added. The addition of the silver nanoparticle brings high capacitance values, due to the corrosion species adsorbed or the corrosion products formed on the carbon steel surface that displayed porous and conducting characteristics [37].

Thus, we have seen that the addition of HEI inhibitor decreases the corrosion rate, but when silver nanoparticles and the inhibitor are added together, an increase in the corrosion rate is observed as reported in the results given above. Similarly, the addition of the Ag nanoparticles to the solution increased the steel corrosion rate. As established above, both HEI and/or Ag nanoparticles had to be adsorbed on the steel surface steel before they can interact with the steel surface and affect its corrosion behavior. In our test system, place due to the presence of two kinds of cationic ions and CO^{2-} anions, a complicated adsorption would take. Firstly, iron carbonate is formed due to the absorption of CO^{2-} ions to form film charging the surface negatively [38, 39]. After that, due to an electrostatic interaction, the HEI ions can be adsorbed on the layer of adsorbed [40, 41]. Later on, a protective film is formed by chemisorption decreasing the steel corrosion rate. However, as shown by the noise measurements, Fig. 5 c, the adsorption of HEI leaves some places uncovered, and local corrosion takes place on the steel surface. When the Ag nanoparticles are added, they can be cooperatively adsorbed on the spare active sites of steel surface, and form galvanic cells with the steel surface, increasing the metal corrosion rate. Micro galvanic cells are formed when the silver nanoparticles are added alone, increasing the corrosion rate also.

4. CONCLUSIONS

A study on the effect of Ag nanoparticles and hydroxyetyl-imidazoline (HEI) on the corrosion inhibition of carbon steel in a CO_2+diesel-saturated 3% NaCl+diesel solution has been carried out. It was found that the addition of Ag nanoparticles alone increased the steel corrosion rate, whereas the addition of the HEI inhibitor decreased it due to its adsorption on to the steel surface and the formation of a protective film. However, when both the Ag nanoparticles and HEI were added together, the corrosion rate was slightly higher than that found with the addition of HEI only, due to the adsorption of the Ag nanoparticles on sites uncovered by the HEI film. The adsorption of the Ag nanoparticles formed galvanic cells with the steel, increasing its corrosion rate.

ACKNOWLEDGEMENTS
Financial support from Consejo Nacional de Ciencia y Tecnologia (CONACYT, México)
(Projects 159898 and 198687) is gratefully acknowledged.

References

1. J. Porcayo-Calderon, L.M. Martínez de la Escalera , J. Canto , M. Casales-Diaz and V.M. Salinas-Bravo, *Int. J. Electrochem. Sci.,* 10 (2015) 3136.
2. F. Farelas and A. Ramirez, *Int. J. Electrochem. Sci*., 5 (2010) 797.
3. S.L. Fu, J.G. Garcia and A.M. Griffin, Proc. From Int. Conference Nace Corrosion/96, paper 21, Corrosion/96, Denver, 1996.
4. P.C. Okafor, X. Liu and Y.G. Zheng, *Corros. Sci*., 51(2009),761.
5. Jingmao Zhao and Guohao Chen, *Electrochim. Acta*, 69 (2012) 1247.

6. 6.T. Hong, Y.H. Sun and W.P. Jepson, *Corros. Sci.*, 44 (2002) 101.
7. F. Farelas, M. Galicia, B. Brown, S. Nesic and H. Castaneda, *Corros. Sci*., 52 (2010) 509.
8. R. Guo, T.Q. Liu and X. Wei, *Colloids Surf. A: Physicochem. Eng. Aspects*, 209 (2002) 37.
9. 9 M. Bouklah, A. Attayibat, B. Hammouti, A. Ramdani, S. Radi and M. Benkaddour, *Appl. Surf. Sci*., 240 (2005) 341.
10. K.F. Khaled, *Appl. Surf. Sci*., 230 (2004) 307.
11. S.T. Keera and M.A. Deyab, *Colloids Surf. A: Physicochem. Eng. Aspects*, 266 (2005), 129.
12. L. Niu, H. Zhang, F.H. Wei, S.X. Wu, X.L. Cao and P.P. Liu, *Appl. Surf. Sci*., 252 (2005) 1634.
13. S.A. Umoren, O. Ogbobe, I.O. Igwe and E.E. Ebenso, *Corros. Sci*., 50 (2008) 1998.
14. T.Y. Soror and M.A. El-Ziady, *Mater. Chem. Phys*., 77 (2003) 697.
15. B.W.A. Sherar, I.M. Power, P.G. Keech, S. Mitlin, G. Southam and D.W. Shoesmith, *Corros. Sci*., 53 (2011) 955.
16. M. Vukovic, V. Cvetkovski and V. Conic, *Corros. Rev*., 27 (2009) 1.
17. B. Little, P. Wagner and F. Mansfeld, *Electrochim. Acta*, 37 (1992) 2185.
18. T.S. Rao, A.J. Kora, B. Anupkumar, S.V. Narasimhan and R. Feser,, *Corros. Sci.*, 47 (2005) 1071.
19. Mahendra Rai, Alka Yadav and Aniket Gade, *Biotechnol. Adv.*, 27 (2009) 76.
20. Ivan Sondi and Branka Salopek-Sondi, , *J. Colloid Interf. Sci.*, 275 (2004) 177.
21. A. Gupta and S. Silver, *Nat. Biotechnol*., 16 (1998) 888.
22. J. S. Kim, E. Kuk and K. N. Yu, *Nanomedicine*, 3 (2007) 95.
23. C. Aymonier, U. Schlotterbeck, L. Antonietti, P. Zacharias, R. Thomann, J.C. Tiller and S. Mecking, *Chem. Commun*., 24 (2002) 3018.
24. S. Ramesh and S. Rajeswari, *Corros. Sci*., 47 (2005) 151.
25. Jingmao Zhao, Hanbing Duan and Ruijing Jiang, *Corros. Sci*., 91 (2015)108.
26. Y.G. Zheng and P.C. Okafor, *Corros. Sci*., 51 (2009) 850.
27. P.H. Stewart and A.B. Campbell, *Can. J. Chem*., 57 (1979) 188.
28. G.W. Walter, *Corros Sci*., 26 (1989) 681.
29. J.L. Mora-Mendoza and S. Turgoose, *Corros. Sci*., 44 (2002) 1223.
30. A. Ikeda, M. Ueda and S. Mukai, Proc, from Int. Conf. Nace Corrosion/83, paper 45, Corrosion/83, Houston, 1983.
31. C. De Waard and D.E. Milliams, *Corrosion* (1975) 177.
32. J.L. Crolet, N. Thevenot and S. Nesic, Proc.From Int. Conference Nace Corrosion/96, paper 3, Corrosion/96, Denver, 1996.
33. P.C. Okafor, E.E. Oguzie, G.E. Iniama, M.E. Ikpi and U.J. Ekpe, *J Pure Appl. Sci*., 14 (2008) 89.
34. K. Hladky and J.L. Dawson, *Corros. Sci*., 22 (1982) 231.
35. J. L. Dawson, A. N. Rothwell, T. G. Walsh, K. Lawson and J. W. Palmer, Proc. From Int. Conference Corrosion 93, Paper No.NACE (1993).
36. Y.J. Tan, S. Bailey and B. Kinsella, *Corros. Sci*., 38 (1996) 1681.
37. M.V. Azghandi, A. Davoodi, G.A. Farzi and A., *Corros. Sci*., 64 (2012) 44.
38. H.Y. Ma, S.H. Chen, B.S. Yin, S.Y. Zhao and X.Q. Liu, *Corros. Sci*., 45 (2003) 867.
39. X.L. Cheng, H.Y. Ma, J.P. Zhang, X. Chen, S.H. Chen and H.Q. Yang, *Corrosion*, 54 (1998) 369.
40. H.Y. Ma, X.L. Cheng, S.H. Chen, G.Q. Li, X. Chen, S.B. Lei and H.Q. Yang, Corrosion, 54 (1998) 634.
41. B. Tribollet, J. Kittel, A. Meroufel, F. Ropital, F. Grosjean and E.M.M. Sutter , *Electrochim. Acta*, 124 (2014) 46.